Journal of Hydrology 613 (2022) 128478

Contents lists available at ScienceDirect

Journal of Hydrology

journal homepage: www.elsevier.com/locate/jhydrol

Research papers

The influence of rainfall interception on the erosive power of raindrops under the birch tree

Anita Zore, Nejc Bezak, Mojca Šraj *

University of Ljubljana, Faculty of Civil and Geodetic Engineering, Jamova cesta 2, 1000 Ljubljana, Slovenia

ARTICLE INFO

This manuscript was handled by Marco Borga, Editor-in-Chief, with the assistance of Kelly Kibler, Associate Editor

Keywords:
Rainfall interception
Throughfall
Drop-size distribution (DSD)
Rainfall erosivity
Optical disdrometer
Kinetic energy

ABSTRACT

Healthy soils are one of the key priorities of the EU Soil Strategy, and soil erosion can present a threat to soils around the world. Rainfall erosivity is the main driver of soil erosion by water. Rainfall interception by vegetation can reduce the erosive power of raindrops, and consequently measures involving vegetation can mitigate soil erosion losses. In this study, the effect of rainfall interception on the erosive power of raindrops under the birch tree in an urban park in the city of Ljubljana is investigated. More than one year of measurements of drop-size distribution using two optical disdrometers placed above and below the birch tree canopy were used to investigate the impact of rainfall interception on the erosive power of raindrops. The number of drops, fall velocity, and drop diameter were, on average smaller below the canopy in comparison to the measurements above the canopy for 20%, 7% and 27%, respectively. This also resulted in a reduction in the rainfall kinetic energy (3% and 30% in the leafless and leafed periods, respectively) and rainfall erosivity (21% and 50% for the leafless and leafed periods, respectively). The results demonstrate that rainfall interception has a significant seasonal influence on the erosive power of raindrops. Therefore, vegetation characteristics should be considered as time-varying rather than constant parameters in soil erosion modelling studies.

1. Introduction

Soil erosion is a raising global threat to agriculture and ecology of oceans and rivers (Borrelli et al., 2020). The main drivers of soil erosion are water and wind, with water erosion studied more frequently than wind erosion (Borrelli et al., 2021), suggesting that water-induced erosion is a major environmental problem worldwide. Rainfall erosivity as a driver of soil erosion is also characterized by large spatial and temporal variability (Bezak et al., 2021a,b,c,d; Bezak et al., 2021a; De Luis et al., 2010; Panagos et al., 2016). While climate change is expected to increase the intensity of the most extreme rainfall events (Burt et al., 2016), which cause the majority of soil erosion, it is important to understand the interaction between rainfall and vegetation, especially because water erosion could increase by up to 50 % in the future (Borrelli et al., 2020). This is especially important because some recent studies have already indicated a positive trend in the rainfall erosivity at continental scales (Bezak et al., 2020). Therefore, nature-based measures such as urban parks or other measures that involve the use of vegetation (Štajdohar et al., 2016; Yao et al., 2015; Zabret and Šraj, 2019a, 2015; Zeng et al., 2021) to cope with flooding and soil erosion will be increasingly applied in the coming decades to reduce the risk of flooding and soil erosion. Therefore, better knowledge of the impact of rainfall interception on rainfall erosivity, which is the main driver of soil erosion, is needed to effectively design and implement nature-based solutions and soil protection measures in the coming decades.

Rainfall interception has a significant influence on the water balance because part of the intercepted rainfall is returned to the atmosphere through evapotranspiration in a relatively short time after the rainfall event, while the other part is infiltrated into the soil and potentially recharges groundwater. Previous studies have demonstrated that tree canopies can intercept notable amounts of rainfall. Geiger et al. (1995) found that deciduous trees intercept between 20 and 25 % of rainfall on average in most cases, while coniferous trees intercept between 20 and 40 % on average. For very low magnitude events or for very extreme events, the amount of intercepted rainfall can be close to 100 % or 0 %, respectively (Bezak et al., 2018; Šraj et al., 2008a; Zabret and Šraj, 2021a). However, it should be noted that the amount of intercepted rainfall is not constant and depends significantly on seasonal characteristics (e.g., phenophase) and meteorological variables (Nanko et al., 2016, 2013,2006; Zabret, 2013; Zabret et al., 2018; Zabret and Šraj,

* Corresponding author.
E-mail address: mojca.sraj@fgg.uni-lj.si (M. Šraj).

https://doi.org/10.1016/j.jhydrol.2022.128478
Received 15 February 2022; Received in revised form 23 August 2022; Accepted 30 August 2022
Available online 21 September 2022

2021a, 2019b).

The microstructure of rainfall, i.e., the number of drops, their diameter and fall velocity, can help us understand the discrete nature of rainfall, which is too often overlooked in soil erosion and rainfall related studies (Uijlenhoet and Sempere Torres, 2006; Zabret et al., 2017). This could be a major drawback as many physical processes at the land surface and in the atmosphere are related to the microstructure of rainfall (Bezak et al., 2021c; Uijlenhoet and Sempere Torres, 2006; Zabret et al., 2017). Rainfall interception by vegetation and soil erosion are two very important processes that are closely related (Carollo et al., 2016; Ciaccioni et al., 2016; Nanko et al., 2020; Petan et al., 2010; Zabret et al., 2017). Rainfall interception by vegetation depends on several factors, such as vegetation characteristics (e.g., canopy storage capacity, tree crown size, vegetation height, leaf properties, etc.) and meteorological factors (e.g., wind speed, air temperature, relative humidity, saturation vapour pressure deficit, microstructure of rainfall, etc.) (Nanko et al., 2013; Nooraei Beidokhti and Moore, 2021; Šraj et al., 2008a; Zabret et al., 2018; Zabret and Šraj, 2021a). Although microstructure of rainfall was reported to be among the most influential meteorological variables related to rainfall interception (Zabret et al., 2018; Zabret and Šraj, 2021a), the number of raindrops, their diameter, and fall velocity are still rarely included in the studies. In order to obtain the data about rainfall microstructure nowadays optical or laser disdrometers are used, which measure the drop size distribution (DSD) and fall velocity of drops (Nanko et al., 2020).

Due to the interaction of rainfall with the canopy, the process of rainfall interception also influences the kinetic energy and therewith the erosive power of raindrops. Rainfall erosivity is usually expressed as a function of kinetic energy of raindrops, which can be determined using rainfall microstructure measurements. There are few studies on rainfall erosivity in the context of rainfall interception (e.g., Cao et al., 2008; Dunkerley, 2020; Frasson and Krajewski, 2011; Goebes et al., 2015; Li et al., 2019; Nanko et al., 2011, 2016,2020; Senn et al., 2020; Shinohara et al., 2018) since high-frequency rainfall and throughfall raindrop size distribution (DSD) data is needed to conduct such a study. Rainfall interception usually reduces rainfall erosivity (e.g., Cao et al., 2008). However, in some cases, leaf dripping can also increase rainfall erosivity (Li et al., 2019; Nanko et al., 2006). Nanko et al. (2006) argued that throughfall, which consists of three drop components, namely free throughfall, drips, and splash droplets has under calm meteorological conditions different DSDs related to the canopy species. They also reported that throughfall usually consists of smaller drops in case of severe vibrations as the consequence of high wind speed. Furthermore, Goebes (2015) has shown that interception itself can reduce the amount of droplets reaching the ground and thus reduce soil erosion, while leaf dripping after the end of the rainfall event can increase the soil erosion.

Soil erosion is an important environmental issue around the globe and has been also recognized within the EU Mission: "A Soil Deal for Europe". Slovenia is no exception, especially because it is among the countries with the highest soil erosion rates in Europe (Panagos et al., 2015b). One of the reasons for these high soil erosion rates is also high rainfall erosivity, which is characteristic for this part of Europe (Bezak et al., 2015; Panagos et al., 2015b). Therefore, the main objective of this study was to investigate the effect of rainfall interception on rainfall erosivity under the birch tree located in an urban park in the capital city of Ljubljana, Slovenia. Specifically, the following scientific questions were investigated: (i) how does the rainfall interception changes the number of drops below the tree canopy compared to measurements above the canopy; (ii) how are the changes in the number of drops, fall velocity, and drop diameter translated into the rainfall kinetic energy and consequently to the rainfall erosivity; (iii) what is the difference between the leafed and leafless period in terms of kinetic energy and rainfall erosivity below and above the vegetation.

2. Data and methods

2.1. Study site

Measurements were conducted at a study site in the southwestern part of the city of Ljubljana, Slovenia (46.04° N, 14.49° E), at 292 m asl. (Zabret et al., 2018, 2017; Zabret and Šraj, 2021a, 2021b, 2019a, 2019b, 2018). The area has subalpine climate with well-defined seasons and is characterized by a temperate oceanic climate (Cfb) according to the Köppen climate classification system (Zabret et al., 2018). The average air temperature for the area is 10.9 °C and the average long-term annual precipitation is 1,362 mm (ARSO, 2021).

The study plot is part of a small urban park with an area of about 600 m^2 (Fig. 1). It is flat and covered with regularly cut grass. It consists of two groups of trees, namely pine trees (*Pinus nigra Arnold*) and birch trees (*Betula pendula Roth.*) in the western part and a clearing in the eastern part of the study site. In this study, we focused only on the birch tree. The observed birch tree is 16.2 m high, with a diameter at breast height (DBH) of 18.3 cm and an upward branch inclination of 53.3° (Zabret and Šraj, 2021b). Birch is characterized by four phenoseasons, namely leafed, leaf-fall, leafless, and leafing. Phenoseasons were defined based on regular measurements of leaf area index (LAI) measured with the LAI-2200 plant canopy analyzer (Li-Cor Inc.) at the study site and compared with official data from the Slovenian Environment Agency at the nearest phenological station, Ljubljana-Bežigrad (ARSO, 2020). Given that there were few events (section 2.2) in the two shorter periods of leaf-fall and leafing, we decided to divide the entire period into only two periods, namely the leafed period, when birch leaves were present and the leafless period, when the canopy was without leaves. The storage capacity of the observed birch tree in leafed period was estimated by Zabret and Šraj (2021b) to be 3.5 mm and the leaf area index (LAI) to be 2.6.

2.2. Measurements

The research is based on the measurements of rainfall microstructure, i.e., raindrop diameter, raindrop velocity, and the number of raindrops over the period of 14 months (24.7.2017 – 24.9.2018) using two laser disdrometers (both OTT Parsivel) placed above and below the birch canopy. The disdrometer above the canopy was installed on the rooftop of the nearby building, having almost the same height as the tree canopies (14.45 m). The measuring area of each disdrometer is 54 cm^2 and the measured data are automatically classified into one of 32 drop diameter classes (ranging from 0.312 mm to 24.5 mm) and 32 velocity classes (ranging from 0.05 m/s to 20.8 m/s), i.e., a total of 1024 classes, as specified by the World Meteorological Organization (WMO). The drop diameters smaller than 0.312 mm, which are outside the measuring range of the instrument, have been assigned to the smallest drop diameter class. Disdrometer is capable of distinguishing eight precipitation types (i.e., drizzle, drizzle/rain, rain, mixed rain/snow, snow, snow grains, sleet, hail); however, in this study we focused only on rain events. The high-frequency measurement time interval of 1 min was used in the study.

Simultaneously, the amount of rainfall was also measured using a tipping bucket (0.2 mm/tip) rain gauge (Onset RG2-M) with an automatic data logger (Onset HOBO Event) located in a clearing in the northeast side of the study site (Fig. 1). Data from this rain gauge was used for control and comparison of rainfall amount as well as to divide measured precipitation into individual rainfall events.

2.3. Methods

Recorded precipitation data was divided into individual rainfall events with at least 6 mm of rain, and separated by periods of at least 6 h without rain, during which the tree canopies were allowed to dry out. The dry time span interval criterion is consistent with the USLE-type

Fig. 1. Photo of the study area, left photo shows the entire plot, while the right photo shows the measuring equipment below the birch canopy. The disdrometer positioned above the canopy is set-up on the building on the left side of the photo, around 50 m from the disdrometer below the canopy.

methodology (e.g., Universal Soil Loss Equation (USLE) and also with the Revised Universal Soil Loss Equation (RUSLE)) (e.g., Renard et al., 1997). In order to consider a large number of events, we decided to use the threshold of 6 mm instead of the 12.7 mm. Petek et al. (2018) performed sensitivity analysis of the USLE-type methodology input criteria and showed that using lower threshold values can increase the number of events while having up to 5–10 % impact on the annual rainfall erosivity. The 6 mm threshold was also used in some other studies that focused on the rainfall interception (Zabret and Šraj, 2019b). Considering the presented criteria (i.e., 6 mm threshold), 83 events were identified during the measurement period. Additionally, we excluded 21 snow events and 4 events due to malfunction of one of a disdrometers. Thus, a total of 58 rainfall events were defined and included in further analysis. Of these, 40 events occurred during the leafed period and 18 during the leafless period. Main characteristics of these 58 events are shown in section 3.1.

In the next step, we calculated the duration and cumulative rainfall amount of individual rainfall events, as well as the corresponding number of drops, their diameter, and their velocity, using raw data from disdrometers placed above and below the canopy. Additionally, we calculated the rainfall intensity *I(dsd)*, kinetic energy of rainfall (KE), and the rainfall erosivity factor R. The R factor was calculated as the product of the KE (Eq. (2)) and I_{30}, which represents the maximum 30-minute rainfall intensity during the rainfall event. The rainfall intensity *I (dsd)* in mm h^{-1} for each time interval *D*t (1/60 h) derived from raindrop size distribution (DSD) measurements was calculated as (Petan et al., 2010):

$$I(dsd) = \frac{\pi}{6 \bullet F \bullet \Delta t} \bullet \sum_i n_i \bullet \frac{1}{D_{b,i} - D_{a,i}} \bullet \int_{D_{a,i}}^{D_{b,i}} D_i^3 dD \quad (1)$$

where *F* is disdrometer measuring area in mm^2, *Dt* is time interval (1/60 h), n_i is the number of detected raindrops in class *i*, D_i is the drop diameter of class i, *Da,i* and *Db,i* are drop size classes limits for specific class in mm.

The 1-minute rainfall kinetic energy per area per time unit *KE(dsd)* in J $m^{-2}h^{-1}$ derived from raindrop size distribution (DSD) measurements was calculated using the following equation (Petan et al., 2010):

$$KE(dsd) = \frac{\pi \bullet \rho}{12 \bullet 10^3 \bullet F \bullet \Delta t} \bullet \sum_i n_i \bullet \frac{1}{D_{b,i} - D_{a,i}} \bullet \int_{D_{a,i}}^{D_{b,i}} D_i^3 dD \bullet \frac{1}{v_{b,i} - v_{a,i}} \bullet \int_{v_{a,i}}^{v_{b,i}} v_i^2 dv, \quad (2)$$

where ρ is water density in kg m^{-3}, v_i is the drop fall velocity of class i, *va,i* and *vb,i* are velocity classes limits for specific class in m s^{-1}. Equation (2) can also be expressed using equation (1). Detailed explanation about the applied methodology can be found in Petan et al. (2010). The methodology and these equations were also used in a recent study that investigated the spatial and temporal variability of rainfall erosivity in Slovenia (Bezak et al., 2021c). Based on the collected and calculated data (i.e., number of drops, fall velocity, kinetic energy, rainfall erosivity) descriptive statistics were calculated and violin plots were used for graphical representation. Additionally, level plots were used for the representation of the disdrometer data for the selected events. Kinetic energy and rainfall erosivity properties are presented in section 3.2. Three events were also studied in detail:

- A low-medium magnitude event with 35 mm of rainfall above the canopy and rainfall duration of around 20 h (September 2017).
- A medium magnitude event with 63 mm of rainfall above the canopy and rainfall duration of around 38 h (November 2017).
- An extreme event with 90 mm of rainfall above the canopy in around 7 h (with a return period of around 25 years) (August 2018).

The selected events also have different ratios of kinetic energy below and above canopy as shown in the Results and discussion section.

3. Results and discussion

3.1. Rainfall interception and drop size distribution (DSD)

The total amount of rainfall detected by the disdrometer below the tree canopy was 1,152 mm, which corresponds to 69 % of rainfall detected by the disdrometer above the canopy (1,669 mm) (Table 1). Thus, we can conclude that the birch tree canopy intercepted 31 % of precipitation during the 58 rainfall events that occurred during the measurement period. This value is comparable to the values previously obtained for the same research area, but for a different time period and

Table 1
The average values and standard deviation of measured variables per event during the measurement period (24.7.2017 – 24.9.2018).

Characteristic	Whole period	Leafless period	Leafed period
Rainfall (P) [mm]	28.8 ± 24.3	25.6 ± 17.9	30.2 ± 26.7
Throughfall (Tf) [mm]	19.9 ± 19.0	19.2 ± 15.7	20.1 ± 20.5
Number of raindrops above the canopy [-]	162,899 ± 152,066	231,514 ± 131,602	132,023 ± 151,976
Number of raindrops below the canopy [-]	129,567 ± 109,457	153,417 ± 106,016	118,835 ± 110,592
Drop diameter above the canopy [mm]	0.92 ± 0.17	0.77 ± 0.10	0.99 ± 0.16
Drop diameter below the canopy [mm]	0.67 ± 0.03	0.66 ± 0.04	0.68 ± 0.03
Drop velocity above the canopy [m/s]	4.06 ± 0.41	3.76 ± 0.30	4.20 ± 0.38
Drop velocity below the canopy [m/s]	3.76 ± 0.03	3.75 ± 0.09	3.77 ± 0.08

for measurements using tipping bucket instruments (Bezak et al., 2018; Šraj et al., 2008b; Zabret et al., 2018; Zabret and Šraj, 2018). More specifically, for the events in the leafed period the average ratio at event scale between througfall and rainfall above the canopy was 59 % with a standard deviation of 13 %. While in the leafless period this ratio at event scale was on average 69 % with a standard deviation of 14 %. Comparison of measured rainfall amount with measurements from a tipping bucket (0.2 mm/tip) rain gauge (Onset RG2-M) located in the nearby clearing demonstrated that disdrometer overestimated total rainfall depth by around 20 %. This finding is consistent with the results of some other studies (Bezak et al., 2013; Bezak et al., 2021c), which found that disdrometer overestimated measured rainfall by about 25 %. This indicates that disdrometer measurements of rainfall can be biased but some of the parameters that can be measured by the disdrometer such as drop fall velocity or diameter can be very useful for the estimation of the kinetic energy. One of the possible reasons for this kind of bias could be an overestimation of large drops (i.e. inhomogeneous laser beam) (Tokay et al., 2013).

A comparison of frequency distribution of measured precipitation and throughfall for the leafless and leafed periods is presented in Fig. 2A. The throughfall amount measured below the birch canopy was 75 % of the precipitation amount during the leafless period and 66 % during the leafed period. The measured values of throughfall below the birch tree canopy are comparable to the results of previous studies under single isolated trees in urban areas, e.g., (Staelens et al., 2008; Xiao et al., 2000; Xiao and McPherson, 2011) as well as with the results from previous periods for the same research area e.g., (Zabret et al., 2018; Zabret and Šraj, 2015). However, we have to consider the fact that rainfall interception is influenced by climatological conditions, which vary from year to year (Zabret and Šraj, 2021a).

The average rainfall intensity calculated using Eq. (1) above the tree canopy for all considered rainfall events was 2.93 mm/h, while this value below the tree canopy was 1.64 mm/h. As we can see, the intensity of precipitation decreased by 44 % on average after it passed the tree canopy. Moreover, at the event scale the average rainfall intensity below the canopy was 55 % and 72 % of the average intensity above the canopy for the leafed and leafless periods, respectively (i.e., with a standard deviation of 16 % in both cases). The results show that precipitation intensity changes to a lesser extent after passing through the birch canopy during the leafless period (Fig. 2B), which can be regarded as an expected result.

During the observation period, the disdrometer detected 162,899 drops per event on average above the tree canopy and 129,567 drops per event below it (Table 1). The results demonstrate that on average 20 % fewer drops were detected below the tree canopy than above. The decrease in the number of drops was more pronounced in the leafless period (34 %) than in the leafed period (10 %), which is also demonstrated in Fig. 3A, where a frequency distribution of the number of raindrops above and below the canopy in both periods is presented. It should be noted that the total number of raindrops above the canopy was higher in the leafless period compared to the leafed period (Table 1 and Fig. 3A), while opposite results were observed for drop diameter and drop velocity (Table 1, Fig. 3B and 3C). Moreover, the detected number of drops can be also affected by the micro-location of the disdrometer beneath the tree canopy (e.g., directly under a branch). Since the measuring area of a disdrometer is only 54 cm^2, this should be considered as a point measurement, while the spatial distribution of throughfall and drop characteristics under the canopy can vary considerably (Zabret and Šraj, 2018). Hence, splashing and dripping below the canopy was more pronounced and uniformly distributed in leafed period (i.e., leaf area index in leafed period is about 2.5 (Zabret and Šraj, 2019a), as drop diameter and drop velocity were also smaller below the canopy than above the canopy (Table 1, Fig. 3B and 3C). On

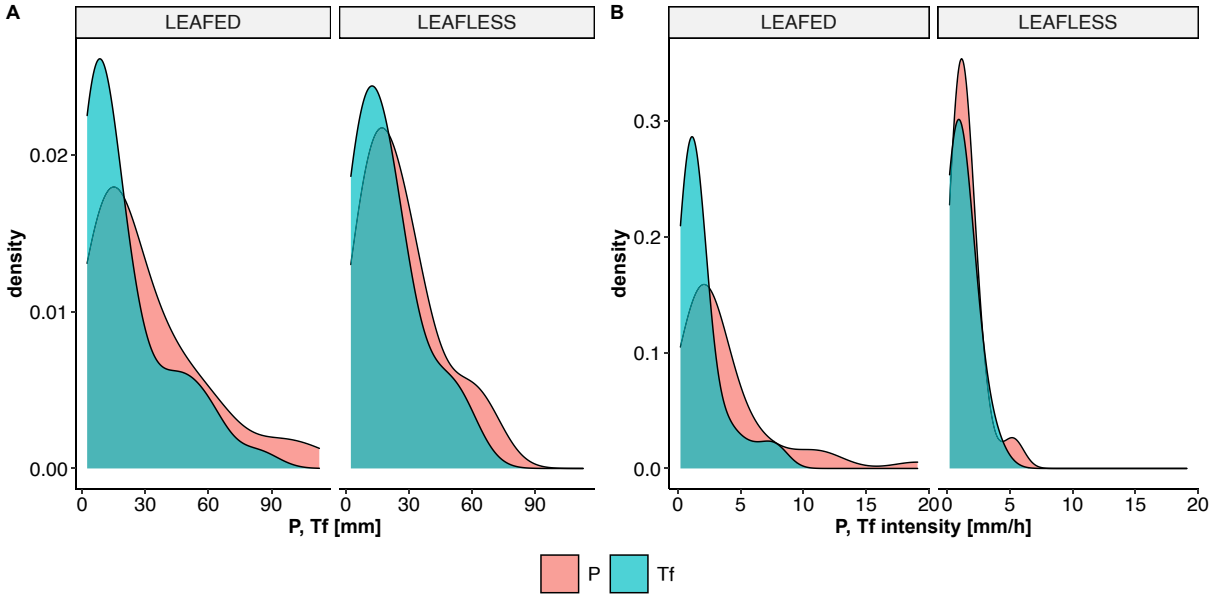

Fig. 2. Kernel density plots of measured precipitation (P) and throughfall (Tf) (A), and corresponding intensity (B) during the leafless and leafed periods.

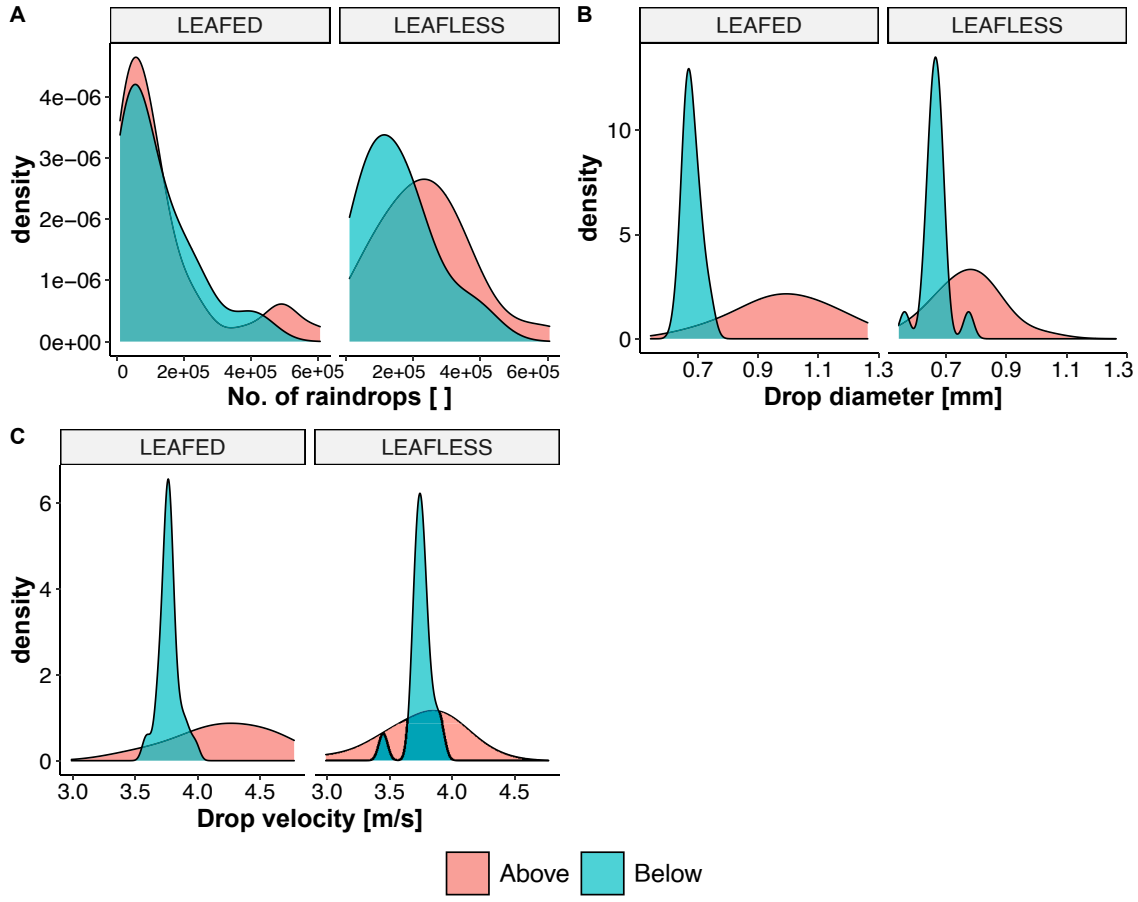

Fig. 3. Kernel density plots of the total number of detected raindrops (A), mean drop diameter (B) and mean drop velocity (C) above and below the tree canopy during the leafless and leafed periods.

the other hand, in the leafless period there is no interception by leaves, while branches can intercept raindrops. It should be noted that stemflow in leafless period was higher compared to the stemflow in leafed period (Zabret and Šraj, 2019a). Thus, it appears that in the leafless period larger percentage of raindrops was intercepted as stemflow compared to the leafed period, which resulted in the reduction of the number of raindrops below the canopy. However, collecting and analysing additional rainfall events both in leafed and leafless period could confirm the reported relationships between the number of events (above and below the tree canopy) in the leafless and leafed periods as the number of events is strongly related to the characteristics of the individual rainfall events. The decrease in the number of drops below the canopy of European beech was also reported by Lüpke et al. (2019) for most of the rainfall events analysed; however, there were some individual events with higher number of drops below the canopy. They indicated that the specific characteristics of drop size distribution can vary significantly even during the individual event. Li et al. (2019) also reported a 16 % decrease in the number of rainfall drops below the canopy of Pinus massoniana Lamb. forest. The detected number of drops has a direct impact on soil erosion because each raindrop, especially large raindrops, can cause soil detachment (Gilley and Finker, 1985). However, besides the number of drops itself, the fall velocity and the drop diameter are the two parameters that control soil detachment (Gilley and Finker, 1985).

Raindrop diameters and velocities were generally higher above the canopy than below the canopy throughout the observation period (Fig. 3B and 3C). The average diameter of raindrops above the tree canopy ranged between 0.54 mm and 1.26 mm during the measurement period. On average, the drop diameter was 0.92 mm (Table 1). On the other hand, the average diameter of raindrops under the birch canopy ranged from 0.56 mm to 0.77 mm, with an average of 0.67 mm (Table 1), representing a 27 % decrease compared to the average diameter of the drops above the tree canopy. The results in Table 1 and Fig. 3B show that the average diameter of raindrops passing through the birch tree canopy decreased, both during the leafless (by 14 %) and leafed (by 31 %) period. However, droplets retain their size under the canopy during the leafless period to a greater extent than during the leafed period (Fig. 3B). This is an expected result, as birch is a deciduous tree, which means that rainfall interception during the leafless period is lower. Also, Nanko et al. (2016), who measured throughfall drop size distributions below the yellow poplar, reported that vegetation period is one of the most influential factors controlling throughfall DSD. They reported that the leafless period had larger sized throughfall drops originating from canopy drip than the leafed period. Furthermore, Nanko et al. (2006) indicated that different tree species generated different sizes of throughfall droplets during the same rainfall event as the consequence of the difference in leaf size and shape among tree species. Additionally, Nanko et al. (2013) demonstrated that throughfall DSD differs between tree species, especially in terms of maximum drop diameter and range of drop diameter. This was also confirmed by Lüpke et al. (2019), who argued that throughfall spectra depends on both tree species and rain event characteristics. They reported a wider diameter range for intense events and a narrower diameter range for lower intensity events.

As raindrop velocity is directly related to the raindrop diameter, the results for the raindrop velocity are very similar (Fig. 3C). According to some previous research (see Mineo et al., 2019), drop velocity strongly depends on the drop diameter for diameters less than 4 mm, while the dependency attenuates for drop diameters ranging from 4 to 6 mm. As

the average drop diameter during the measurement period was about 1 mm, a strong relationship between mean drop diameter and mean drop velocity was expected, especially in case of measurements above the canopy. An exponential dependence was found between the two variables in both, the leafed (Pearson correlation coefficient 0.88) and leafless (Pearson correlation coefficient 0.99) periods. In case of measurements below the tree canopy, a relatively high dependence was also observed in the leafless period (Pearson correlation coefficient 0.93), while no dependence was found in the leafed period (Pearson correlation coefficient 0.08). As expected, the dependence of drop diameter and drop velocity was stronger in the leafless period and the dependency is quite similar above and below the tree canopy. We also evaluated the performance of the equation proposed by Carollo and Ferro (2015) (Carollo et al., 2016) for estimating terminal velocity based on measured drop diameter. With respect to the relationship between leafless (Pearson correlation coefficient was 0.98 and 0.92 above and below the canopy, respectively) and leafed (Pearson correlation coefficient was 0.88 and −0.09 above and below the canopy, respectively) periods and measurements above and below the canopy similar conclusions can be drawn as in the case of measured average drop diameter and drop velocity. During the period of measurements, the average velocity of raindrops per event above the birch canopy varied between 2.99 m/s and 4.77 m/s. The average velocity of the drops per event was 4.06 m/s. The average velocity of raindrops below the birch canopy ranged from 3.45 m/s to 3.99 m/s, averaging 3.76 m/s, which is 7 % lower compared to the average velocity of droplets above the tree canopy. Lower velocity of throughfall drops was also reported by Nanko et al. (2020), who argued that a decrease in velocity can be attributed to the insufficient fall distance from the canopy to the floor to reach terminal velocity. The average velocity of raindrops decreased when passing through the birch canopy, both during the leafless (less than 1 %) and leafed (by 10 %) periods, which followed the results of the raindrop diameters. Thus, it is clear that rainfall interception not only affects the number of drops reaching the ground (i.e., an average decrease of 20 %) but also decreases fall velocity (i.e., an average decrease of 7 %) and drop diameter (i.e., an average decrease of 27 %). These numbers also indicate that the corresponding kinetic energy and rainfall erosivity should be lower below the tree canopy compared to the characteristics in the open.

3.2. Kinetic energy and rainfall erosivity

The rainfall kinetic energy derived from the raindrop size distribution (DSD) measurements using Eq. (2) ranged from 0.28 MJ/ha to 15.4 MJ/ha. The results presented in Fig. 4A indicate that the kinetic energy of raindrops was maintained during the leafless period as they passed through the canopy (the difference was 3 %), while it decreased by an average of 30 % during the leafed period. Similar can also be observed for the rainfall erosivity factor R, which largely depends on the duration of the event, the size and velocity of the raindrops as well as the phenophase. It should be noted that KE and R are closely related (i.e., $R = KE*I_{30}$); however, R factor is often used by the USLE-type soil erosion models such as USLE, RUSLE or RUSLE2. As we can see from Fig. 4B the rainfall erosivity factor R decreased by 21 % and 50 % on average after the raindrops passed the canopy during the leafless and leafed periods, respectively. Thus, we can conclude that the birch canopy during the leafed period reduced the erosivity factor R by 29 % compared to the leafless period.

The ratio between rainfall erosivity factor R above and below the tree canopy ranged from 0.3 to 15.0 (both extreme values were determined in the leafed period) (Fig. 5). Moreover, it can be found that the average ratio between R above and below the tree canopy is 63 % lower in the leafless period than in the leafed period (Fig. 5). The seasonal variation of the ratio between rainfall erosivity above and below the tree canopy is shown in Fig. 6A. The ratio was less than 1 (i.e., rainfall interception did not decrease rainfall erosivity) for only 4 precipitation events (2 in leafless and 2 in leafed period). More specifically, these four events can be explained by an increase in rainfall erosivity due to dropping of larger drops or multiple smaller drops from the canopy during and after the event (Table 2; Fig. 6). These four events all had more than 12 mm of rainfall, which means that the storage canopy capacity was exceeded (Zabret and Šraj, 2021a). It is clear that the summer months are characterized by larger rainfall erosivity, the rainfall events also have a higher average rainfall intensity (Fig. 6B), and rainfall interception leads to a more significant decrease in the rainfall erosivity (Fig. 6A). Fig. 7 shows an example of a medium magnitude event with ratio of rainfall erosivity above and below the canopy smaller than 1 that occurred in November 2017 during the leafless period (Table 2). As we can see, the drop size distribution is fairly even throughout the event, both above and below the canopy. Hence, also the average drop diameter and

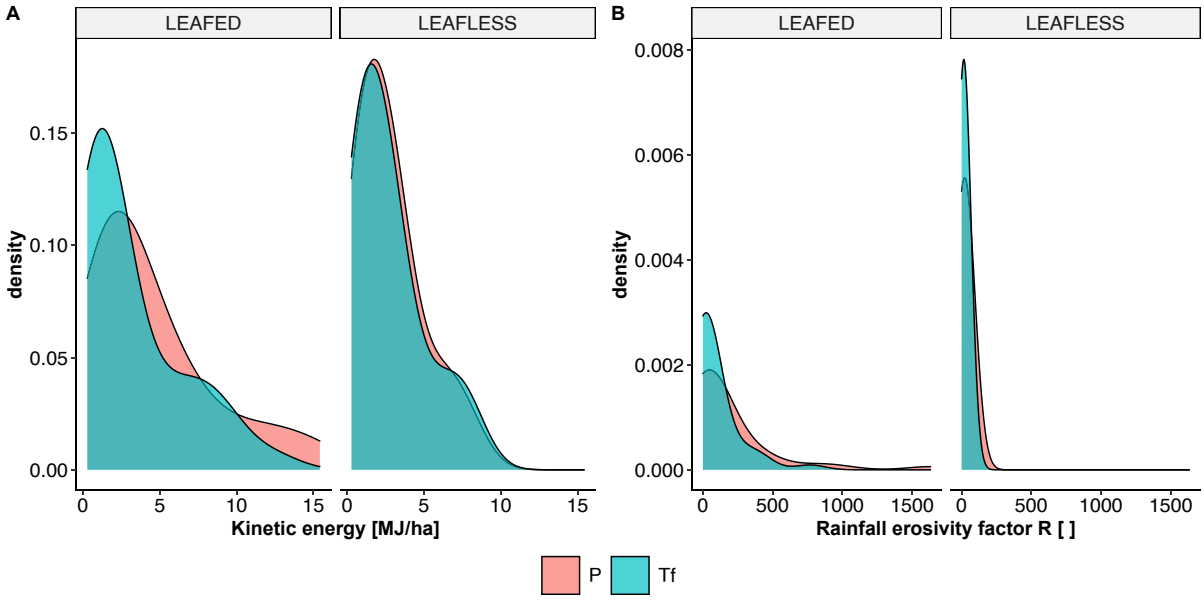

Fig. 4. Kernel density plots of the kinetic energy (A) and rainfall erosivity factor R (B) above and below the tree canopy during the leafless and leafed periods, respectively.

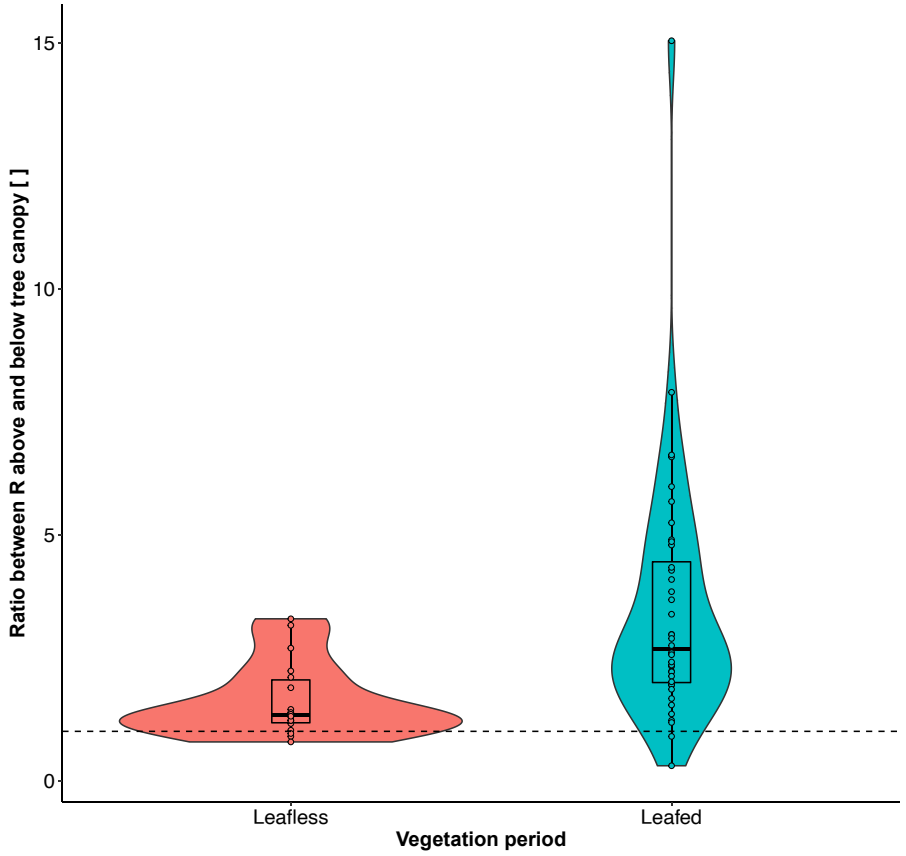

Fig. 5. The ratio between R above the tree canopy and R below the tree canopy during the leafless and leafed periods, respectively.

average drop velocity are relatively similar above and below the canopy (Table 2). Rainfall erosivity below the canopy (i.e., around 10 %) was slightly higher than rainfall erosivity above the tree canopy (i.e., around 50 MJ*mm*ha^{-1}*h^{-1}). A similar relationship can be seen for the rainfall kinetic energy (Table 2), while I_{30} values are relatively similar below and above the canopy (i.e., around 7.7 mm/h). On the other hand, Fig. 8 shows an example of a low-medium magnitude rainfall event that occurred in September 2017 during the leafed period. The number of raindrops detected during this event was obviously much larger above the canopy than below it (Fig. 8). Rainfall erosivity above the canopy was about 2 times higher than the rainfall erosivity below the canopy (i.e., 15 MJ*mm*ha^{-1}*h^{-1}) (Table 2). The kinetic energy above the canopy was also higher than below the canopy, although the difference was not very significant (Table 2). In case of this event, also the I_{30} below the canopy was around 40 % lower compared to intensity above the canopy, which was equal to around 7.7 mm/h (Table 2). Thus, the vegetation intercepted a large portion of the raindrops and reduced their kinetic energy and rainfall intensities (i.e., I_{30}), especially compared to the leafless period and the rainfall event that is shown in Fig. 7, where there was almost no reduction in I_{30}. It should be noted that the mean I_{30} above and below the canopy is equal to 18 mm/h and 12.5 mm/h, respectively. While the maximum values of the I_{30} for the detected rainfall events are equal to 78 mm/h and 105 mm/h below and above the canopy, respectively. Hence, it can be seen that specific ratios between rainfall intensities, kinetic energy and consequently of the erosive power of raindrops depend on characteristics of rainfall event and can vary significantly from one event to another.

Furthermore, a detailed analysis of the extreme magnitude rainfall event with a kinetic energy of 15.4 MJ/ha was also conducted (Table 2; Fig. 9). The event was recorded on August 14, 2018, when a summer storm occurred. The event had the highest kinetic energy among all 58 events considered above and below the tree canopy. It lasted for 7.1 h. During this time, 90.7 mm of rain fell above the birch canopy and 60.7 mm was recorded below it. The rainfall intensity was 12 mm/h and the throughfall intensity was 8 mm/h. Raindrops above the canopy with an average diameter of 1.1 mm reached an average drop velocity of 4.5 m/s, while the average diameter of raindrops below the canopy decreased to 0.7 mm and drop velocity to 3.6 m/s (Table 2). The kinetic energy of the event decreased from 15.4 MJ/ha above the tree canopy to 9.8 MJ/ha below it, which is 36 %. The rainfall erosivity factor R was 1632 MJ*mm*ha^{-1}*h^{-1} above the tree canopy and decreased to 769 MJ*mm*ha^{-1}*h^{-1} below it. In this case, rainfall interception by the tree canopy reduced the rainfall erosivity factor by 53 %. Moreover, it can be seen that during the extreme event, which occurred in leafed period, the interception by vegetation lead to a lagged dripping from leaves after the peak rainfall intensity above the canopy (Fig. 9). Moreover, the rainfall erosivity of this event can be regarded as relatively extreme and is within the range of the annual rainfall erosivity at some European locations (e.g., parts of Central or Eastern Europe) (Panagos et al., 2015a). Furthermore, for the entire period of measurements used in this study, this specific event contributed to around 22 % of the total rainfall erosivity, which was equal to around 7,200 MJ*mm/ha*h. The total recorded rainfall erosivity can be regarded as relatively extreme, but it should be noted that it includes two summer seasons. Hence, this is in accordance to the results presented by Bezak et al. (2021) who showed that around 5–10 events are needed to account for 50 % of the annual rainfall erosivity at this part of Europe. Bezak et al. (2021) also showed that inequality described with Gini coefficient in Slovenia is among the highest in Europe. On the other hand, Fig. 7 and Fig. 8 present two examples of low to medium intensity rainfall events that are associated with much smaller rainfall erosivity values compared to the summer event that is shown in Fig. 9.

These findings are consistent with the results of previous studies. For example, Cao et al. (2008) reported that erosivity is reduced mainly by

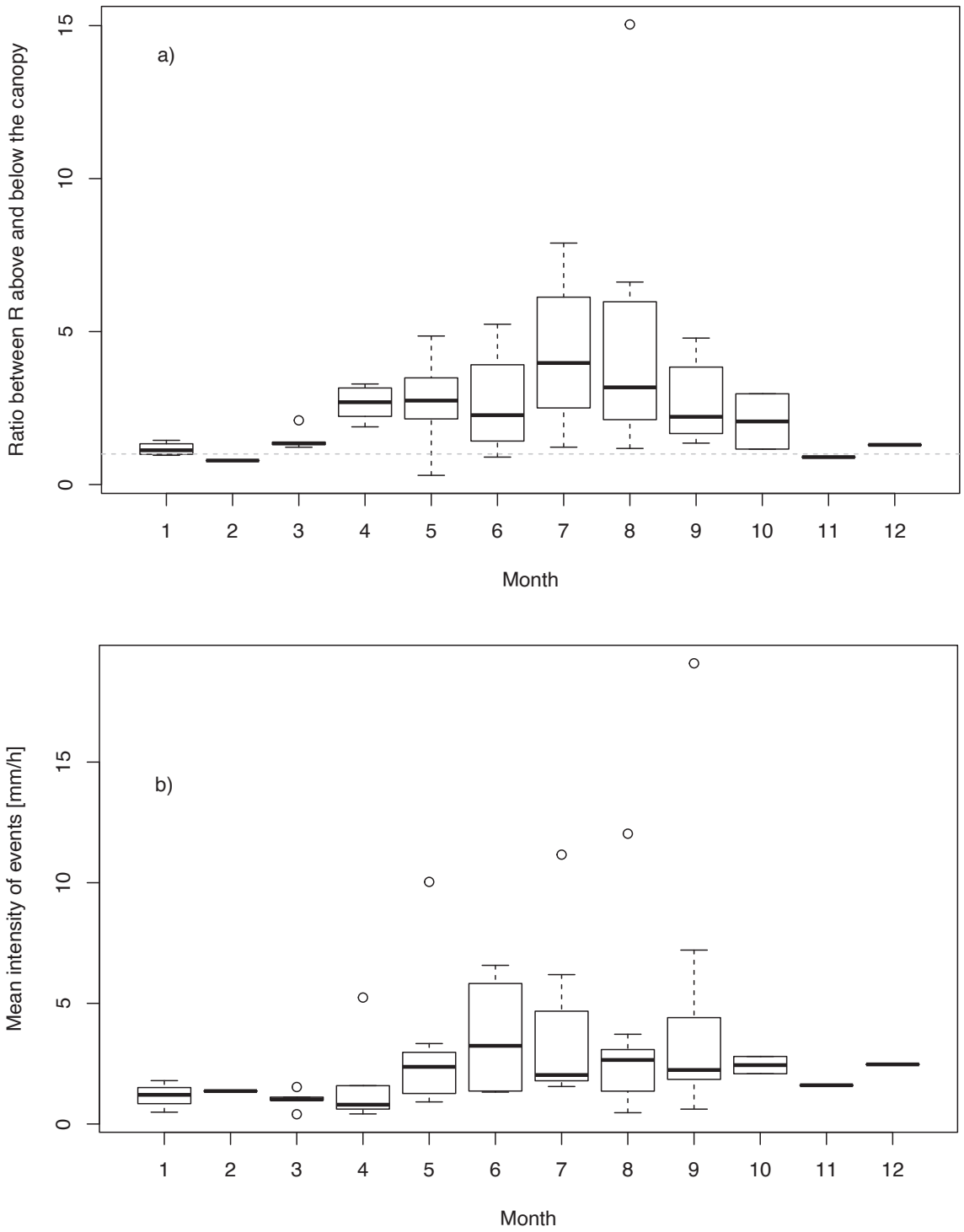

Fig. 6. Monthly variations of the ratio between the rainfall erosivity factor R calculated above and below the tree canopy (A) and the mean rainfall intensity of the events (B). Box-plots with potential outliers are shown.

rainfall interception. On the other hand, some authors (Goebes, 2015; Nanko et al., 2020, 2006) indicated that leaf dripping may also increase rainfall erosivity in some cases. Li et al. (2019) found that kinetic energy below the canopy of Pinus massoniana Lamb. forest is reduced at higher rainfall intensity and the effect is reversed at lower rainfall intensity.

3.3. Connection of the rainfall interception impact to USLE-type methodology

In the scope of the USLE-type methodology (Renard et al., 1997), the vegetation effect is considered using the dimensionless crop cover and management factor C. Thus, different values for the crop cover and management factor can be found in the literature for a given land use type (Bezak et al., 2015; Esetlili et al., 2014; Panagos et al., 2015b; Renard et al., 1997). For example, Thapa (2020) used a value of 0.03 for

Table 2
Basic characteristics of three selected rainfall events below and above the canopy that are shown in Figs. 7–9.

Event	Fig. 7 (November 2017)	Fig. 8 (September 2017)	Fig. 9 (August 2018)
Duration [h]	37.8	18.5	7.1
Rainfall amount above and below canopy [mm]	63.2 and 50.9	35.0 and 24.6	90.7 and 60.7
Average drop diameter above and below canopy [mm]	0.8 and 0.7	0.6 and 0.7	1.1 and 0.7
Average drop velocity above and below canopy [m/s]	3.8 and 3.7	3.4 and 3.8	4.5 and 3.6
Kinetic energy above and below canopy [MJ/ha]	6.5 and 7.2	3.3 and 3.2	15.4 and 9.8
Maximum 30-min intensity (I_{30}) above and below canopy [mm/h]	7.6 and 7.7	7.7 and 4.7	105.8 and 78.4
Rainfall erosivity below and above canopy [MJ*mm*ha^{-1}*h^{-1}]	49.8 and 55.5	25.1 and 15.1	1631.5 and 769.2

forest and a value of 0.45 for bare land and 0.01 for grassland. On the other hand, Bezak et al. (2015) used a value of 0.002 for forest and a value of 0.004 for pastures. Other studies also report different values for the crop cover and management factor, and most studies do not distinguish between forest types (e.g., deciduous and coniferous tree species). Thus, it is clear that such assessments have a high degree of subjectivity. While most studies apply a constant value of the crop cover and management factor for soil erosion calculations (Bezak et al., 2015; Esetlili et al., 2014; Thapa, 2020) it is clear that the effect of vegetation depends on numerous meteorological factors and vegetation characteristics as shown in this study. Therefore, the use of a constant value of factor C in the context of soil erosion assessments using the USLE-type methodology may lead to uncertain results. It should be noted that the RUSLE manual provides detailed description of how time-varying parameters should be calculated (e.g., half-month values) (Renard et al., 1997). Therefore, additional investigations using high-frequency measurements below and above different vegetation species should be conducted to evaluate the accuracy of soil erosion calculations using the USLE-type methodology and to estimate the potential error in cases where a constant value of parameter C is used in the calculations. Therefore, the soil erosion modelling community (Bezak et al., 2021b; Borrelli et al., 2021) should focus on better and more frequent consideration of varying (or seasonal dependent) dimensionless crop cover and management factor and more precise estimation of rainfall erosivity. It should be noted that Nearing et al. (2017) have pointed out that the empirical equations used by RUSLE to estimate rainfall erosivity may underestimate erosivity while providing a reasonable estimate of the spatial or temporal differences in erosivity. Hence, the use of the original

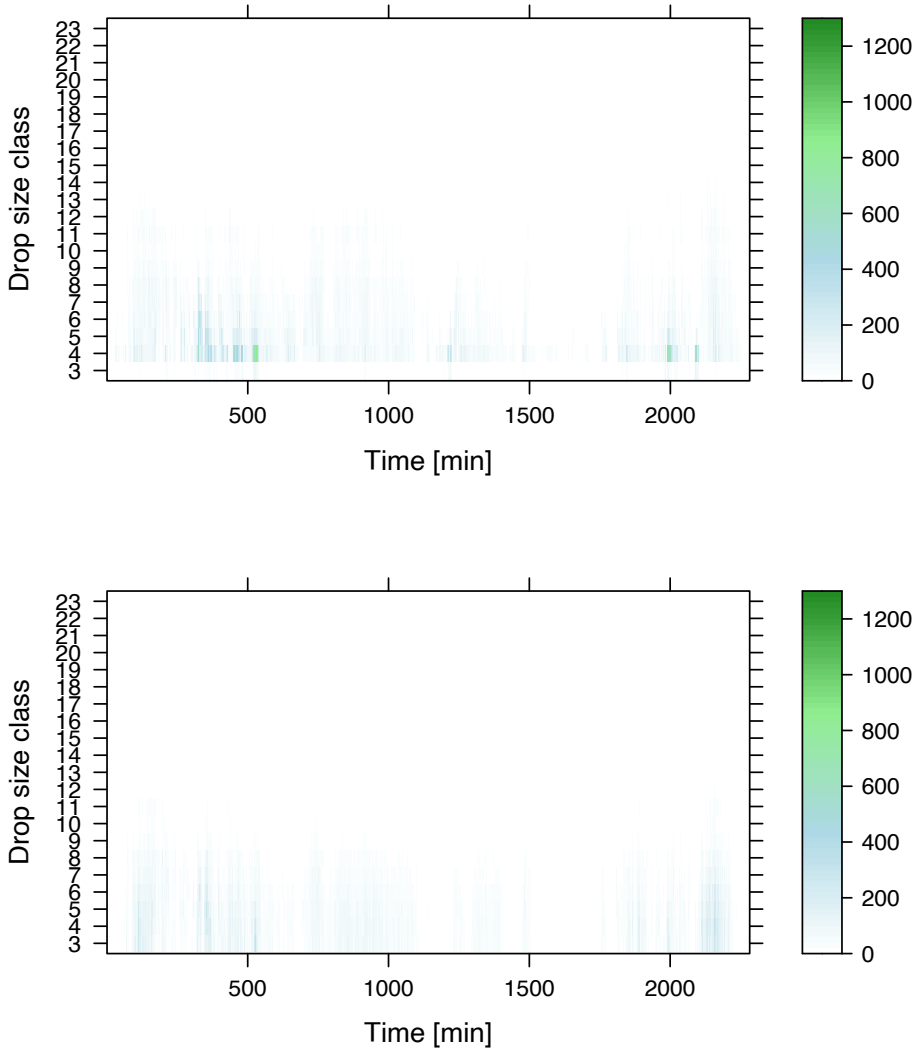

Fig. 7. Number of detected raindrops per diameter class (classes 3–23 are shown) for the rainfall event that occurred on the 6th and 7th of November 2017. The upper and lower panels show the number of detected raindrops above and below the tree canopy, respectively.

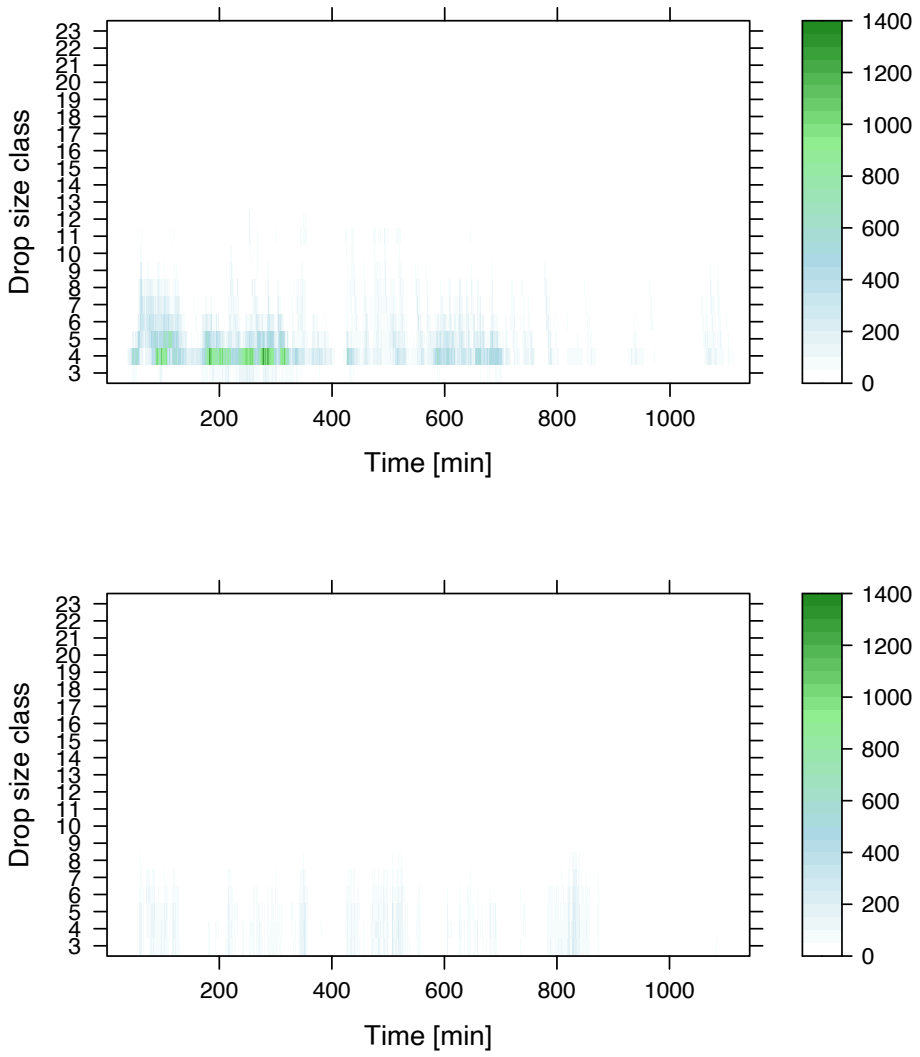

Fig. 8. Number of detected raindrops per diameter class (classes 3–23 are shown) for the rainfall event that occurred on the 12th of September 2017. The upper and lower panels show the number of detected raindrops above and below the tree canopy, respectively.

USLE or RUSLE2 energy equation is suggested (Nearing et al., 2017). Moreover, it should also be noted that rainfall erosivity is an empirically-based index and that actual soil erosion rates depend on numerous factors (Nearing et al., 2017). For example, Nearing et al. (2017) pointed out that kinetic energy of raindrops is not the driving force behind the rill erosion in some cases. Additionally, one should be aware that there are several limitations related to the USLE-type models as discussed by Alewell et al. (2019). Nevertheless, USLE-type models are the most commonly applied for soil erosion assessment worldwide (Borrelli et al., 2021).

4. Conclusions

This study presents the results of 14-month measurements using optical disdrometers placed below and above the birch tree canopy in an urban park in Ljubljana, Slovenia. Based on the results presented, it can be concluded that:

(i) Rainfall interception by birch yielded a decrease in the number of raindrops, fall velocity and their diameter below the canopy compared to the rainfall in the open. The average decrease in these characteristics for the 58 rainfall events was 20 %, 7 %, and 27 % for the number of drops, fall velocity and drop diameter, respectively.

(ii) This also resulted in reduced kinetic energy of rainfall that was not intercepted by the canopy, and consequently reduced rainfall erosivity in general. Moreover, the differences between the kinetic energy (3 % and 30 % in the leafless and leafed periods, respectively) and rainfall erosivity (21 % and 50 % for the leafless and leafed periods, respectively) below and above the tree canopy can be considered significant and are clearly not constant throughout the year, but depends on seasonal characteristics, meteorological conditions and vegetation properties. Therefore, the decrease in the rainfall erosivity due to rainfall interception can vary significantly from one rainfall event to another. Moreover, it was shown that few events can contribute to the majority of the annual rainfall erosivity. This indicates that high inequality exists in the magnitudes of erosive rainfall events.

(iii) There was a clear difference in the number of drops, fall velocity, drop diameter, kinetic energy and rainfall erosivity in the leafless and leafed periods. For example, the average ratio between R above and below the tree canopy is 63 % lower in the leafless period than in the leafed period.

Therefore, it is clear that vegetation cover such as trees have an important effect on the reduction of the kinetic energy of raindrops hitting the soil and thus on soil erosion rates by reducing rainfall erosivity. Therefore, nature-based solutions that involve vegetation such

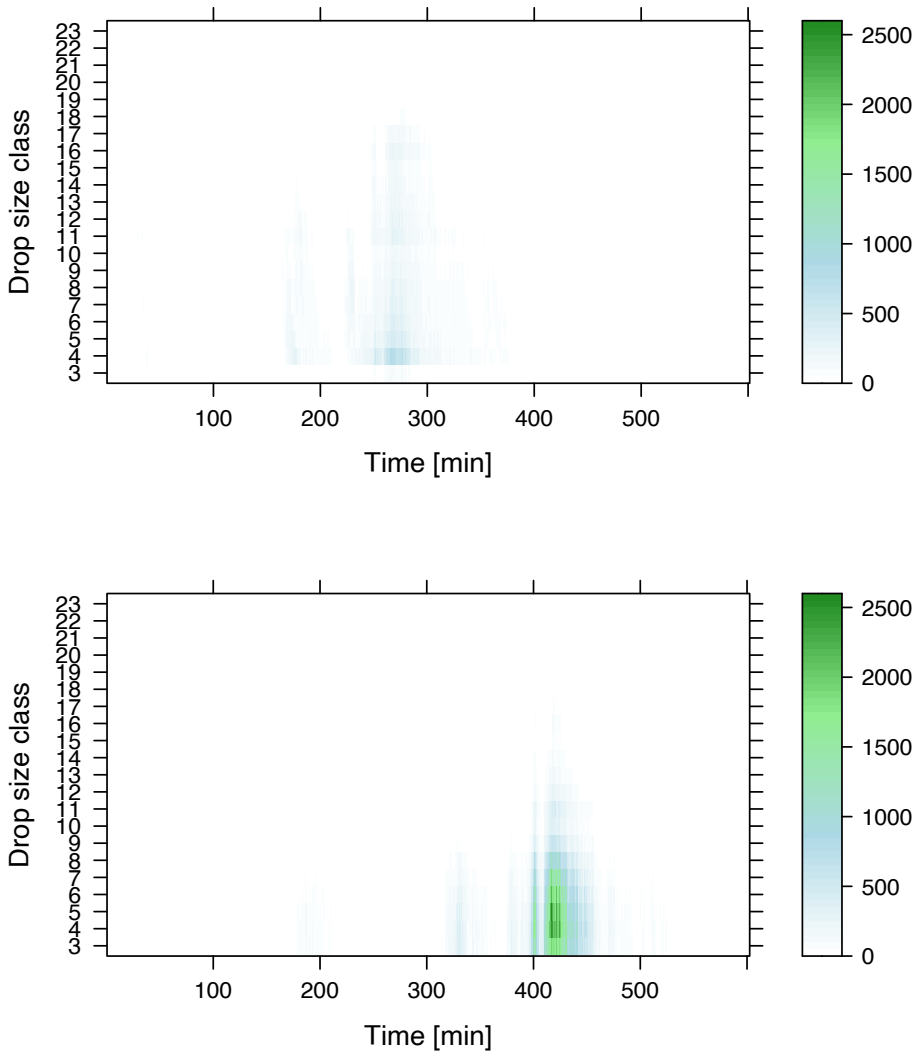

Fig. 9. Number of detected raindrops per diameter class (classes 3–23 are shown) for the rainfall event that occurred on the 14th of August 2018. The upper and lower panels show the number of detected raindrops above and below the tree canopy, respectively.

as trees not only have a positive impact on the microclimate, flood risk control, but also have a significant impact on reducing the kinetic energy of rainfall and thus soil erosion. This is especially important as climate change is expected to increase the intensity of the most extreme rainfall events and trees could be used to cope with potential increase in soil erosion rates in the coming decades. Moreover, soil erosion modelling community should more frequently apply time-varying crop-management factor rather than using constant factor in relation to applying USLE-type models.

More detailed investigations regarding the drop size distribution characteristics will be performed in future since the experimental plot in the city of Ljubljana was upgraded with measurements of drop size distribution characteristics also below the pine tree canopy.

Authors contributions

A. Zore: data validation, data analysis, results interpretation. N. Bezak: formulation of the aims of the study, visualisation, results interpretation, writing – review and editing. M. Šraj: conceptualization, formulation of the aims of the study, data visualisation, results interpretation, writing – original draft, review and editing.

CRediT authorship contribution statement

Anita Zore: Validation. **Nejc Bezak:** Visualization, Writing – review & editing. **Mojca Šraj:** Conceptualization, Writing – original draft, Writing – review & editing.

Declaration of Competing Interest

The authors declare that they have no known competing financial interests or personal relationships that could have appeared to influence the work reported in this paper.

Data availability

Data will be made available on request.

Acknowledgments

The results of the study are part of the research Programme P2-0180: “Water Science and Technology, and Geotechnical Engineering: Tools and Methods for Process Analyses and Simulations, and Development of Technologies” that is financed by the Slovenian Research Agency (ARRS). The conducted research work was also done in the scope of the UNESCO Chair on Water-related Disaster Risk Reduction and CELSA

project “Interception experimentation and modelling for enhanced impact analysis of nature based solutions”. Critical and useful comments of three anonymous reviewers and associate editor greatly improved this work.

References

Alewell, C., Borrelli, P., Meusburger, K., Panagos, P., 2019. Using the USLE: Chances, challenges and limitations of soil erosion modelling. Int. Soil Water Conserv. Res. 7, 203–225. https://doi.org/10.1016/j.iswcr.2019.05.004.

ARSO, 2020. Agrometeorology [WWW Document]. Phenol. data.

ARSO, 2021. Measurements archive [WWW Document]. Clim. Slov. Tables.

Bezak, N., Šraj, M., Rusjan, S., Kogoj, M., Vidmar, A., Sečnik, M., Brilly, M., Mikoš, M., 2013. Comparison between two adjacent experimental torrential watersheds: Kuzlovec and Mačkov graben. Acta Hydrotechnica 26, 85–97.

Bezak, N., Rusjan, S., Petan, S., Sodnik, J., Mikoš, M., 2015. Estimation of soil loss by the WATEM/SEDEM model using an automatic parameter estimation procedure. Environ. Earth Sci. 74, 5245–5261. https://doi.org/10.1007/s12665-015-4534-0.

Bezak, N., Zabret, K., Šraj, M., 2018. Application of copula functions for rainfall interception modelling. Water (Switzerland) 10, 995. https://doi.org/10.3390/w10080995.

Bezak, N., Ballabio, C., Mikoš, M., Petan, S., Borrelli, P., Panagos, P., 2020. Reconstruction of past rainfall erosivity and trend detection based on the REDES database and reanalysis rainfall. J. Hydrol. 590, 125372 https://doi.org/10.1016/j.jhydrol.2020.125372.

Bezak, N., Borrelli, P., Panagos, P., 2021a. A first assessment of rainfall erosivity synchrony scale at pan-European scale. Catena 198, 105060. https://doi.org/10.1016/j.catena.2020.105060.

Bezak, N., Mikoš, M., Borrelli, P., Alewell, C., Alvarez, P., Anache, J.A.A., Baartman, J., Ballabio, C., Biddoccu, M., Cerdà, A., Chalise, D., Chen, S., Chen, W., De Girolamo, A. M., Gessesse, G.D., Deumlich, D., Diodato, N., Efthimiou, N., Erpul, G., Fiener, P., Freppaz, M., Gentile, F., Gericke, A., Haregeweyn, N., Hu, B., Jeanneau, A., Kaffas, K., Kiani-Harchegani, M., Villuendas, I.L., Li, C., Lombardo, L., López-Vicente, M., Lucas-Borja, M.E., Maerker, M., Miao, C., Modugno, S., Möller, M., Naipal, V., Nearing, M., Owusu, S., Panday, D., Patault, E., Patriche, C.V., Poggio, L., Portes, R., Quijano, L., Rahdari, M.R., Renima, M., Ricci, G.F., Rodrigo-Comino, J., Saia, S., Samani, A.N., Schillaci, C., Syrris, V., Kim, H.S., Spinola, D.N., Oliveira, P.T., Teng, H., Thapa, R., Vantas, K., Vieira, D., Yang, J.E., Yin, S., Zema, D.A., Zhao, G., Panagos, P., 2021b. Soil erosion modelling: A bibliometric analysis. Environ. Res. 197, 111087 https://doi.org/10.1016/j.envres.2021.111087.

Bezak, N., Mikoš, M., Borrelli, P., Liakos, L., Panagos, P., 2021c. An in-depth statistical analysis of the rainstorms erosivity in Europe. Catena 206. https://doi.org/10.1016/j.catena.2021.105577.

Bezak, N., Petan, S., Mikoš, M., 2021d. Spatial and Temporal Variability in Rainfall Erosivity Under Alpine Climate: A Slovenian Case Study Using Optical Disdrometer Data. Front. Environ. Sci. 9, 1–16. https://doi.org/10.3389/fenvs.2021.735492.

Borrelli, P., Robinson, D.A., Panagos, P., Lugato, E., Yang, J.E., Alewell, C., Wuepper, D., Montanarella, L., Ballabio, C., 2020. Land use and climate change impacts on global soil erosion by water (2015–2070). Proc. Natl. Acad. Sci. U. S. A. 117, 21994–22001. https://doi.org/10.1073/pnas.2001403117.

Borrelli, P., Alewell, C., Alvarez, P., Anache, J.A.A., Baartman, J., Ballabio, C., Bezak, N., Biddoccu, M., Cerdà, A., Chalise, D., Chen, S., Chen, W., De Girolamo, A.M., Gessesse, G.D., Deumlich, D., Diodato, N., Efthimiou, N., Erpul, G., Fiener, P., Freppaz, M., Gentile, F., Gericke, A., Haregeweyn, N., Hu, B., Jeanneau, A., Kaffas, K., Kiani-Harchegani, M., Villuendas, I.L., Li, C., Lombardo, L., López-Vicente, M., Lucas-Borja, M.E., Märker, M., Matthews, F., Miao, C., Mikoš, M., Modugno, S., Möller, M., Naipal, V., Nearing, M., Owusu, S., Panday, D., Patault, E., Patriche, C.V., Poggio, L., Portes, R., Quijano, L., Rahdari, M.R., Renima, M., Ricci, G.F., Rodrigo-Comino, J., Saia, S., Samani, A.N., Schillaci, C., Syrris, V., Kim, H.S., Spinola, D.N., Oliveira, P.T., Teng, H., Thapa, R., Vantas, K., Vieira, D., Yang, J.E., Yin, S., Zema, D.A., Zhao, G., Panagos, P., 2021. Soil erosion modelling: A global review and statistical analysis. Sci. Total Environ. 146494. https://doi.org/10.1016/j.scitotenv.2021.146494.

Burt, T., Boardman, J., Foster, I., Howden, N., 2016. More rain, less soil: Long-term changes in rainfall intensity with climate change. Earth Surf. Process. Landforms 41, 563–566. https://doi.org/10.1002/esp.3868.

Cao, Y., Ouyang, Z.Y., Zheng, H., Huang, Z.G., Wang, X.K., Miao, H., 2008. Effects of forest plantations on rainfall redistribution and erosion in the red soil region of Southern China. L. Degrad. Dev. 19, 321–330.

Carollo, F.G., Ferro, V., 2015. Modeling rainfall erosivity by measured drop-size distributions. J. Hydrol. Eng. 20 https://doi.org/10.1061/(ASCE)HE.1943-5584.0001077.

Carollo, F.G.F.G., Ferro, V., Serio, M.A.M.A., 2016. Estimating rainfall erosivity by aggregated drop size distributions. Hydrol. Process. 30, 2119–2128. https://doi.org/10.1002/hyp.10776.

Ciaccioni, A., Bezak, N., Rusjan, S., 2016. Analysis of Rainfall Erosivity Using Disdrometer Data At Two Stations in Central Slovenia. Acta Hydrotechnica 29, 89–101.

De Luis, M., González-Hidalgo, J.C., Longares, L.A., 2010. Is rainfall erosivity increasing in the Mediterranean Iberian peninsula? L. Degrad. Dev. 21, 139–144. https://doi.org/10.1002/ldr.918.

Dunkerley, D., 2020. A Review of the Effects of Throughfall and Stemflow on Soil Properties and Soil Erosion. In: Van Stan, J.T., Gutmann, E., Friesen, J. (Eds.), PrecipitAtion PArtitioning by VegetAtion: A GlobAl Synthesis. Springer International Publishing, pp. 183–213. https://doi.org/10.1007/978-3-030-29702-2.

Esetlili, M.T., Ozen, F., Kurucu, Y., Kaya, U., 2014. Agroecological aspect of olive cultivation. J. Environ. Prot. Ecol. 15, 1810–1822.

Frasson, R.P.de M., Krajewski, W.F., 2011. Characterization of the drop-size distribution and velocity-diameter relation of the throughfall under the maize canopy. Agric. For. Meteorol. 151, 1244–1251. https://doi.org/10.1016/j.agrformet.2011.05.001.

Geiger, R., Arog, R.H., Todhunter, P., 1995. The climate near the ground. Friedr. Vieweg & Sohn, Braunschweig/ Wiesbaden.

Gilley, E.J., Finker, C.S., 1985. Estimating Soil Detachment Caused by Raindrop Impact. Trans. ASAE 28, 140–146. https://doi.org/10.13031/2013.32217.

Goebes, P., 2015. Mechanisms of soil erosion in subtropical forests of China: effects of biodiversity, species identity, tree architecture and spatial variability on erosivity. Univ. Tübingen.

Goebes, P., Seitz, S., Kühn, P., Li, Y., Niklaus, P.A., von Oheimb, G., Scholten, T., 2015. Throughfall kinetic energy in young subtropical forests: Investigation on tree species richness effects and spatial variability. Agric. For. Meteorol. 213, 148–159. https://doi.org/10.1016/j.agrformet.2015.06.019.

Li, G., Wan, L., Cui, M., Wu, B., Zhou, J., 2019. Influence of canopy interception and rainfall kinetic energy on soil erosion under forests. Forests 10. https://doi.org/10.3390/f10060509.

Lüpke, M., Leuchner, M., Levia, D., Nanko, K., Shin'ichi, I., Menzel, A., 2019. Characterization of differential throughfall drop size distributions beneath European beech and Norway spruce. Hydrol. Process. 33, 3391–3406. https://doi.org/10.1002/hyp.13565.

Mineo, C., Ridolfi, E., Moccia, B., Russo, F., Napolitano, F., 2019. Assessment of rainfall kinetic-energy-intensity relationships. Water (Switzerland) 11, 1994. https://doi.org/10.3390/w11101994.

Nanko, K., Tanaka, N., Leuchner, M., Levia, D.F., 2020. Throughfall Erosivity in Relation to Drop Size and Crown Position: A Case Study from a Teak Plantation in Thailand, in: Levia, D.F., Carlyle-Moses, D.E., Iida, S., Michalzik, B., Nanko, Kazuki (Eds.), Forest-Water Interactions. Springer Nature Switzerland, pp. 279–298. doi:10.1007/978-3-030-26086-6_12.

Nanko, K., Hotta, N., Suzuki, M., 2006. Evaluating the influence of canopy species and meteorological factors on throughfall drop size distribution. J. Hydrol. 329, 422–431. https://doi.org/10.1016/j.jhydrol.2006.02.036.

Nanko, K., Onda, Y., Ito, A., Moriwaki, H., 2011. Spatial variability of throughfall under a single tree: Experimental study of rainfall amount, raindrops, and kinetic energy. Agric. For. Meteorol. 151, 1173–1182. https://doi.org/10.1016/j.agrformet.2011.04.006.

Nanko, K., Watanabe, A., Hotta, N., Suzuki, M., 2013. Physical interpretation of the difference in drop size distributions of leaf drips among tree species. Agric. For. Meteorol. 169, 74–84. https://doi.org/10.1016/j.agrformet.2012.09.018.

Nanko, K., Hudson, S.A., Levia, D.F.D.F., 2016. Differences in throughfall drop size distributions in the presence and absence of foliage. Hydrol. Sci. J. 61, 620–627. https://doi.org/10.1080/02626667.2015.1052454.

Nearing, M.A., Yin, S.-Q., Borrelli, P., Polyakov, V.O., 2017. Rainfall erosivity: An historical review. Catena 157, 357–362. https://doi.org/10.1016/j.catena.2017.06.004.

Nooraei Beidokhti, A., Moore, T.L., 2021. The effects of precipitation, tree phenology, leaf area index, and bark characteristics on throughfall rates by urban trees: A meta-data analysis. Urban For. Urban Green. 60, 127052 https://doi.org/10.1016/J.UFUG.2021.127052.

Panagos, P., Ballabio, C., Borrelli, P., Meusburger, K., Klik, A., Rousseva, S., Tadić, M.P., Michaelides, S., Hrabalíková, M., Olsen, P., Beguería, S., Alewell, C., 2015a. Rainfall erosivity in Europe. Sci. Total Environ. 511, 801–814. https://doi.org/10.1016/j.scitotenv.2015.01.008.

Panagos, P., Borrelli, P., Poesen, J., Ballabio, C., Lugato, E., Meusburger, K., Montanarella, L., Alewell, C., 2015b. The new assessment of soil loss by water erosion in Europe. Environ. Sci. Policy 54, 438–447. https://doi.org/10.1016/j.envsci.2015.08.012.

Panagos, P., Ballabio, C., Borrelli, P., Meusburger, K., 2016. Spatio-temporal analysis of rainfall erosivity and erosivity density in Greece. Catena 137, 161–172. https://doi.org/10.1016/j.catena.2015.09.015.

Petan, S., Rusjan, S., Vidmar, A., Mikoš, M., 2010. The rainfall kinetic energy-intensity relationship for rainfall erosivity estimation in the mediterranean part of Slovenia. J. Hydrol. 391, 314–321. https://doi.org/10.1016/j.jhydrol.2010.07.031.

Petek, M., Mikoš, M., Bezak, N., 2018. Rainfall erosivity in Slovenia: Sensitivity estimation and trend detection. Environ. Res. 167, 528–535. https://doi.org/10.1016/j.envres.2018.08.020.

Renard, K.G., Foster, G.R., Weesies, G.A., McCool, D.K., Yoder, D.C., 1997. Predicting Soil Erosion by Water: A Guide to Conservation Planning with the Revised Universal Soil Loss Equation (RUSLE), Agricultural Handbook. U.S. Department of Agriculture, Washington.

Senn, J.A., Fassnacht, F.E., Eichel, J., Seitz, S., Schmidtlein, S., 2020. A new concept for estimating the influence of vegetation on throughfall kinetic energy using aerial laser scanning. Earth Surf. Process. Landforms 45, 1487–1498. https://doi.org/10.1002/hyp.13565.

Shinohara, Y., Ichinose, K., Morimoto, M., Kubota, T., Nanko, K., 2018. Factors influencing the erosivity indices of raindrops in Japanese cypress plantations. Catena 171, 54–61. https://doi.org/10.1016/j.catena.2018.06.030.

Šraj, M., Brilly, M., Mikoš, M., 2008a. Rainfall interception by two deciduous Mediterranean forests of contrasting stature in Slovenia. Agric. For. Meteorol. 148, 121–134.

Šraj, M., Lah, A., Brilly, M., 2008b. Meritve in analiza prestreženih padavin navadne breze (Betula pendula Roth.) in rdečega bora (Pinus sylvestris L.) v urbanem okolju. Gozdarski Vestn. 9, 406–433.
Staelens, J., De Schrijver, A., Verheyen, K., Verhoest, N.E.C., 2008. Rainfall partitioning into throughfall, stemflow, and interception within a single beech (Fagus sylvatica L.) canopy: influence of foliation, rain event characteristics, and meteorology. Hydrol. Process. 22, 33–45. https://doi.org/10.1002/hyp.6610.
Štajdohar, M., Brilly, M., Šraj, M., 2016. The influence of sustainable measures on runoff hydrograph from an urbanized drainage area. Acta Hydrotechnica 29, 145–162.
Thapa, P., 2020. Spatial estimation of soil erosion using RUSLE modeling: a case study of Dolakha district, Nepal. Environ. Syst. Res. 9, 15. https://doi.org/10.1186/s40068-020-00177-2.
Tokay, A., Petersen, W.A., Gatlin, P., Wingo, M., 2013. Comparison of raindrop size distribution measurements by collocated disdrometers. J. Atmos. Ocean. Technol. 30, 1672–1690. https://doi.org/10.1175/JTECH-D-12-00163.1.
Uijlenhoet, R., Sempere Torres, D., 2006. Measurement and parameterization of rainfall microstructure. J. Hydrol. 328, 1–7. https://doi.org/10.1016/j.jhydrol.2005.11.038.
Xiao, Q., McPherson, G.G., 2011. Rainfall interception of three trees in Oakland, California. Urban Ecosyst. 14, 755–769. https://doi.org/10.1007/s11252-011-0192-5.
Xiao, Q., McPherson, E.G., Ustin, S.L., Grismer, M.E., Simpson, J.R., 2000. Winter rainfall interception by two mature open-grown trees in Davis, California. Hydrol. Process. 14, 763–784. https://doi.org/10.1002/(SICI)1099-1085(200003)14:4<763::AID-HYP971>3.0.CO;2-7.
Yao, L., Chen, L., Wei, W., Sun, R., 2015. Potential reduction in urban runoff by green spaces in Beijing: A scenario analysis. Urban For. Urban Green. 14, 300–308. https://doi.org/10.1016/J.UFUG.2015.02.014.
Zabret, K., 2013. The influence of tree characteristics on rainfall interception. Acta Hydrotechnica 26, 99–116.
Zabret, K., Šraj, M., 2019a. Rainfall Interception by Urban Trees and Their Impact on Potential Surface Runoff. Clean - Soil, Air, Water 47, 1800327. https://doi.org/10.1002/clen.201800327.
Zabret, K., Šraj, M., 2019b. Evaluating the influence of rain event characteristics on rainfall interception by urban trees using multiple correspondence analysis. Water (Switzerland) 11, 2659. https://doi.org/10.3390/W11122659.
Zabret, K., Šraj, M., 2021a. Relation of influencing variables and weather conditions on rainfall partitioning by birch and pine trees. J. Hydrol. Hydromechanics 69, 456–466. https://doi.org/10.2478/johh-2021-0023.
Zabret, K., Šraj, M., 2021b. How Characteristics of a Rainfall Event and the Meteorological Conditions Determine the Development of Stemflow: A Case Study of a Birch Tree. Front. For. Glob. Chang. 4, 1–13. https://doi.org/10.3389/ffgc.2021.663100.
Zabret, K., Šraj, M., 2015. Can Urban Trees Reduce the Impact of Climate Change on Storm Runoff? Urbani izziv 26, S165–S178. https://doi.org/10.5379/urbani-izziv-en-2015-26-supplement-011.
Zabret, K., Rakovec, J., Mikoš, M., Šraj, M., 2017. Influence of Raindrop Size Distribution on Throughfall Dynamics under Pine and Birch Trees at the Rainfall Event Level. Atmosphere (Basel). 8, 240. https://doi.org/10.3390/atmos8120240.
Zabret, K., Šraj, M., 2018. Spatial variability of throughfall under single birch and pine tree canopies. Acta Hydrotechnica 31, 1–20. https://doi.org/10.15292/acta.hydro.2018.01.
Zabret, K., Rakovec, J., Šraj, M., 2018. Influence of meteorological variables on rainfall partitioning for deciduous and coniferous tree species in urban area. J. Hydrol. 558, 29–41. https://doi.org/10.1016/j.jhydrol.2018.01.025.
Zeng, J., Lin, G., Huang, G., 2021. Evaluation of the cost-effectiveness of Green Infrastructure in climate change scenarios using TOPSIS. Urban For. Urban Green. 64, 127287 https://doi.org/10.1016/J.UFUG.2021.127287.